CHAPTER 3

CONCEPTUAL DESIGN AND SIMULATION STUDY*

*Part of this work has been published as:

Manpuran Mahto and Pradip Kumar Jain, "Design and Simulation Study of the HPM Oscillator—Reltron," *IEEE Transactions on Plasma Science*, vol. 44, pp. 743–748, 2016.

CONCEPTUAL DESIGN AND SIMULATION STUDY

3.1. Introduction

High power microwave (HPM) sources are widely used for various defense and civilian applications, and considerable research activities have been aroused in the last few decades. Reltron is one of the highly efficient and compact HPM sources which does not require external DC magnetic field. It is a slow-wave microwave tube and relatively a new member of the klystron family with few differences. First, in reltron double velocity modulation occurs in the RF cavity to bunch the electron beam and second, the bunched beam is reaccelerated through a post-acceleration gap towards the output section of the device [Soh *et al.* (2012)]. The device mode of operation is TM_{01} and the RF output extraction is directly through a rectangular waveguide in its fundamental TE_{10} mode without any mode converter [Miller *et al.* (1992)]. A 3D schematic view of a reltron is shown in Fig. 3.1 indicating all the subassemblies of the device. Miller *et al*. have obtained an RF output power of ~200MW with an extraction efficiency of ~32 % with the first experimental reltron [Miller *et al.* (1992)]. Kim *et al*. have reported a 3D PIC simulation of a reltron without grids in the modulation using thermionic emission and obtained a 38.3 MW RF output power with 52.7% efficiency using "MAGIC" code [Kim *et al.* (2009)]. Soh *et al*. carried out PIC simulation for a dual mode reltron using "MAGIC" code and reported an RF output power of 128 MW with 35% efficiency in the TM_{010} and TM_{110} modes [Soh *et al.* (2012)].

In the present chapter, an expression for start oscillation current of reltron is derived. A device design methodology of the reltron is presented in detail and subsequently used to design a reltron. A reltron with explosive electron emission

process is simulated using a commercial 3D PIC code "CST Particle Studio". Electromagnetic (EM) simulation, in the absence of electron beam, is carried out to find the mode and frequency of excitation as well as EM field present inside the RF cavity of the device. To estimate the overall performance of the device, such as operating frequency, RF output power, and efficiency, PIC simulation in the presence of the electron beam is also carried out.

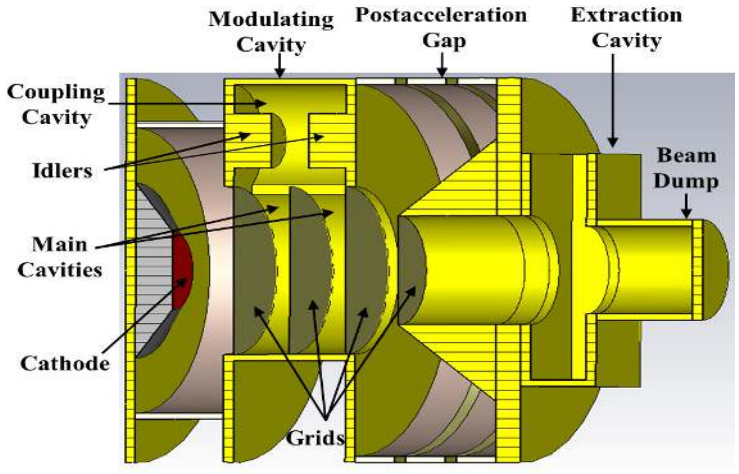

Figure 3.1: 3D schematic diagram of a reltron.

3.2. Description of the Start Oscillation Current

In this section, the start oscillation current in reltron device has been analyzed. The RF electric field (E) inside the modulation cavity under the $\pi/2$ mode of operation is defined as [Miller *et al.* (1992)]:

$$E = \begin{matrix} -E_0 \sin(\omega t + \theta) & 0 < z < g \\ E_0 \sin(\omega t + \theta) & g < z < 2g \end{matrix}, \qquad (3.1)$$

where E_0 is the peak field amplitude, θ is the initial phase condition for the electric field and g is the grid spacing in the modulation cavity. Since the gap voltage in the modulation cavity is very small, the electron beam bunching is dominated by the space

charge forces and the fundamental current in the first grid spacing ($0 \leq z \leq g$) is given by [Friedman *et al.* (1988)]:

$$I_1 = jM(V_{gap} / Z)\sin(\alpha\mu\theta_1), \tag{3.2}$$

where M is the coupling coefficient in the modulation cavity, V_{gap} is the gap voltage developed in the modulation cavity, and Z is the impedance of the cavity defined by [Friedman *et al.* (1984)]:

$$Z = \frac{\gamma_0^3 \beta_0^2 mc^2}{e I_0}, \tag{3.3}$$

where e and m are the charge and mass of the electron, respectively, c is the speed of the light, I_0 is the DC beam current. The initial relativistic mass factor γ_0 and RF phase propagation constant β_0 are given by [Friedman *et al.* (1988)]:

$$\gamma_0 = (1-\beta_0^2)^{-1/2} \quad \text{and} \quad \beta_0 = v_0 / c \quad , \tag{3.4}$$

where v_0 is the initial velocity of electrons given by the injector kinetic energy. The terms α, μ and θ_1 are defined as [Friedman *et al.* (1988)]:

$$\alpha = I_0 / I_s \gamma_0^3 \beta_0, \tag{3.5}$$

$$\mu = (\alpha^2 + \alpha / \gamma_0^2)^{1/2} / \alpha\beta_0, \tag{3.6}$$

and

$$\theta_1 = \omega\delta g / \beta_0 c \ . \tag{3.7}$$

Here, $\delta = \beta_0^2 / (\beta_0^2 - \alpha)$ and I_s is the normalized threshold current which depends on the cathode radius (r_c) and main cavity radius (r_m) as [Friedman *et al.* (1988)]:

$$I_s = \frac{2\pi\varepsilon_0 m_0 c^3}{e\ln(r_m / r_c)}. \tag{3.8}$$

The current flowing in the second grid spacing ($g \le z \le 2g$) is modified as [Friedman *et al.* (1988)]:

$$I_2 = jM(V_{gap}/Z)[\sin(\alpha\mu\theta_2) + (2\omega g/Z)\sin(\alpha\mu\theta_1)\sin(\alpha\mu(\theta_2 - \theta_1))], \tag{3.9}$$

where $\theta_2 = 2\omega\delta g / \beta_0 c$. The power coupled from the beam to the cavity is:

$$P_c = \frac{1}{2} M I_2 V_{gap} \tag{3.10}$$

and the power dissipated out from the cavity is:

$$P_d = \frac{V_{gap}^2}{2R}. \tag{3.11}$$

For energy balance, the energy stored in the cavity (E_S) is the difference between the power coupled in (P_c) and the power dissipated out (P_d) from the RF cavity as [Carlsten and Haynes (1996)]:

$$\frac{dE_s}{dt} = \frac{1}{2} V_{gap} I_2 M - \frac{V_{gap}^2}{2R},$$

$$\Rightarrow \quad \frac{dE_s}{dt} = \frac{1}{2} V_{gap} I_2 M - \frac{V_{gap}^2}{2Q(R/Q)}, \tag{3.12}$$

where Q is RF cavity quality factor. Equations (3.3) (3.9) and (3.12) provide:

$$\frac{dE_s}{dt} = \frac{V_{gap}^2}{2(R/Q)} \times H_{gr}, \tag{3.13}$$

where H_{gr} is the normalized growth rate, described as:

$$H_{gr} = \left[\frac{jM^2\delta}{Z} \left(\frac{R}{Q} \right) - \frac{1}{Q} \right]. \tag{3.14}$$

Substituting (3.3) in (3.14) yields:

$$H_{gr} = \left[\frac{je\delta M^2 I_0}{\gamma_0^3 \beta_0^2 mc^2} \left(\frac{R}{Q} \right) - \frac{1}{Q} \right]. \tag{3.15}$$

The expression for the gap voltage can be written as:

$$V_{gap} = V_{beam} e^{\omega t H_{gr}/2}, \tag{3.16}$$

where V_{beam} is the total beam voltage applied to the cavity. To set up the oscillation condition, the device growth rate (3.15) should be positive, which leads to:

$$QI_0 \geq \frac{\gamma_0^3 \beta_0^2 mc^2}{je\delta M^2} \left(\frac{R}{Q} \right)^{-1} \quad . \tag{3.17}$$

Hence, the start oscillation current for the device becomes:

$$I_{start} = \frac{\gamma_0^3 \beta_0^2 mc^2 V_{beam}}{je\delta M^2 R}, \tag{3.18}$$

where the shunt impedance (R) is given by the product of quality factor (Q) and geometric factor (R/Q). To build the oscillation the beam current must exceed this current, otherwise oscillation will not sustain and gradually dies out.

3.3. Design Methodology

A reltron device is designed in accordance with the various design constraints. The process of designing a reltron includes operating mode corresponding to the RF interaction structure, operating frequency, electron beam parameters and mode of extraction at the output cavity, etc. The operating mode of reltron is typically selected as the TM_{01} and the RF cavity dimensions are primarily determined by the device oscillation frequency. The various steps involved in the design procedure are discussed

here. The radius r_m of the main cavities of the modulation cavity can be determined as:

$$r_m = \frac{\chi_{mn} c}{2\pi f_c}, \tag{3.19}$$

where χ_{mn} is the eigenvalue, as the root of Bessel function, which is the TM mode dispersion relation of the cylindrical waveguide system and is equal to 2.405 for the TM_{01} mode. c is the speed of light and f_c is the cylindrical waveguide section cutoff frequency.

In the equivalent circuit analysis of modulation cavity of reltron, the equivalent capacitance per unit length of the main cavities and coupling cavity are selected as $2C_0$ and C_0, respectively. Since the capacitance is proportional to the square of the cavity radius, following relationships are understood [Soh *et al.* (2010)]:

$$2C_0 \propto r_m^2, \tag{3.20}$$

and

$$C_0 \propto r_r^2, \tag{3.21}$$

where r_r is radius of coupling cavity. Expressions (3.20) and (3.21) can be rewritten as:

$$\frac{r_m}{r_r} = \sqrt{2} \Rightarrow r_r \approx \frac{2}{3} r_m. \tag{3.22}$$

Therefore, the radius of the coupling cavity is approximately chosen as two-third of the main cavities. When the electrons enter the modulation cavity, they undergo velocity modulation and lose their most of the kinetic energy in the middle of the grid spacing ($z = g/2$), where they experience maximum retardation. The optimum distance can be expressed in the form [Soh (2012)]:

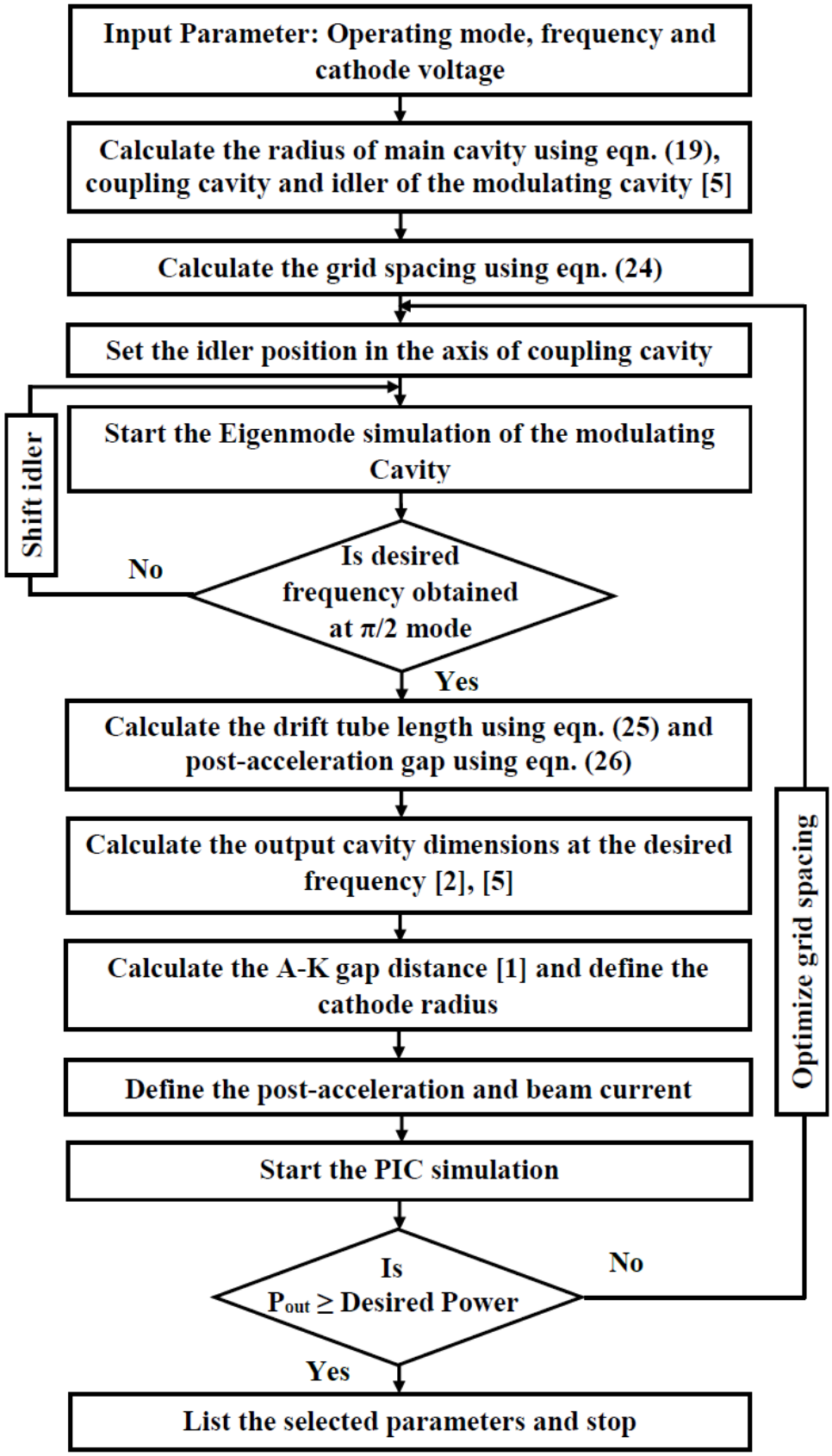

Figure 3.2: Flowchart describing the reltron design procedure.

$$k_z z = \frac{\pi}{2}, \tag{3.23}$$

where k_z (= $2\pi/\lambda$) is the wavenumber and λ (= v_0/f) is the wavelength due to electron motion. Substituting the value of k_z as $2\pi/\lambda$ and z as $g/2$ in expression (3.23) provides us a relationship for the grid spacing in the modulation cavity as:

$$g = \frac{v_0}{2f}. \tag{3.24}$$

Miller *et al*. [Miller *et al.* (1992)] have performed several experiments as well as numerical calculations and established that the anode-cathode gap should be approximately 1.1 times the value of grid spacing g (d_{ak} = 1.1g) to ensure virtual cathode formation in the modulation cavity of the device. If the anode-cathode gap is less than this spacing, due to the absence of the virtual cathode formation, intense beam bunching does not take place which in turn will reduce the RF interaction and device efficiency.

At the output end, where the RF signal is to be extracted from the electron beam, the slow space charge waves with positive group velocity propagate in the forward direction, leaving the output port. But the slow space charge waves with negative group velocity present here will propagate in the backward direction. To prevent this backward wave propagation, a drift tube section whose cutoff frequency is much less than the device oscillation frequency is used. Generally a long drift tube is used to prevent the backward propagation because a wave attenuates within a few wavelength. A drift tube length of a few wavelength is sufficient to attenuate these waves and can be obtained as [Soh (2012)]:

$$L_{DT} = \frac{n\pi}{k_z}, \tag{3.25}$$

where n = 3/2, 5/2, 7/2, … , are the current density peaks in the middle of the extraction cavity to ensure the maximum extraction. The length of the post-acceleration gap can be calculated as [Soh (2012)]:

$$L_{PA} = L_{DT} + \frac{L_{OC}}{2}, \tag{3.26}$$

where L_{OC} is the length of the extraction cavity along the axial direction. The extraction cavity is a standard rectangular waveguide designed to get the output power in TE_{10} mode. The detailed design procedure of reltron is shown in Fig. 2 and the design specification are listed in Table 3.1.

3.4. Device Simulation

In order to understand the device operating mechanism and performance evaluation of the reltron, the device is designed based on the methodology described in the previous section, and simulated using commercial PIC code "CST Particle Studio" [*User's Manual*, CST (2014)]. For the device simulation, first, the reltron device structure, as shown in Fig. 3.1 is modeled as per the property of the structure material, electrical and dimensional parameters. Then EM simulation of the modulation cavity is performed in the absence of the electron beam to ensure the resonating frequency and the EM field profile in the structure. Then, the reltron structure is simulated in the presence of electron beam (hot condition) to observe the oscillation frequency, RF output power and efficiency of the device. The detailed procedure used in the design and simulation of the reltron using CST Eigenmode Solver for beam absent case and CST Particle Studio for beam present case is shown in Fig. 3.2.

Table 3.1: Design specifications of the reltron [Miller *et al.* (1992)]

(a) Device electrical specification	
Operating frequency (f)	2.75 GHz
Total beam voltage (V_{beam})	850 kV
Cathode voltage (V_{ak})	100 kV
Post-acceleration voltage (V_{pa})	750 kV
Beam Current (I_{b})	750 A
(b) Structural Parameters	
Main cavity radius (r_m)	38.27 mm
Coupling cavity radius (r_r)	25.51 mm
Idler radius	12.75 mm
Grid spacing (g)	18.70 mm
A-K gap spacing (d_{ak})	20.50 mm
Drift tube length (L_{DT})	44.80 mm
Post-acceleration gap (L_{PA})	53.30 mm

3.4.1. Eigenmode Simulation

A For performing the beam absent simulation, the modulation cavity is modeled using the design parameters described in Table 3.1. CST Eigenmode Solver is used for beam absent simulation to study its electromagnetic behavior. The modulation cavity has three pillbox cavities so it must have three resonant frequencies corresponding to three different modes, *i. e.*, 0, π/2 and π [Miller *et al.* (1992)]. The electric field patterns of these three modes are shown in Fig. 3.3. It can be observed from Fig. 3.3(a) that in 0-mode, the electric fields in the main cavities as well as in the coupling cavity are in the same direction, and it resonates at 2.57 GHz. In π-mode shown in Fig. 3.3(c), resonates at 2.96 GHz, the electric fields in the main cavities are in the same phase, but the electric field in the coupling cavity is in opposite phase to the main cavities. While in

the π/2 mode as shown in Fig. 3.3(b) has no electric field in the coupling cavity and in the main cavities the electric fields are in opposite phase which resonates at 2.76 GHz.

In reltron, operation occurs in π/2 mode, and if an electron which arrives the first main cavity at a time when the oscillating field in the pillbox cavity will decelerate the electron, as a result, the cavity EM fields will grow, by conservation of energy. The electrons which are injected half-cycle later will be accelerated in both cavities. Since, the decelerated electrons employ more time in the main cavities than the accelerated electrons on an average, the net energy transfer is from the beam to the cavity fields. This situation is classically unstable and gives rise to the space charge instability in the device. This instability is responsible for the virtual cathodes formation, thereby, faster RF signal growth and maximum energy transfer [Miller *et al.* (1992)].

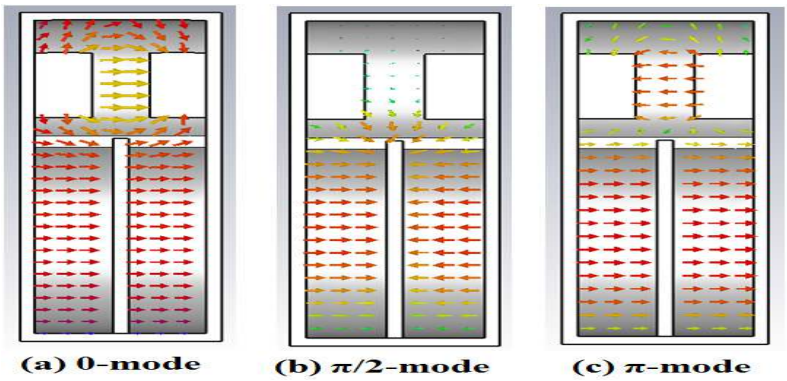

Figure 3.3: Electric field patterns in (a) 0-mode (b) π/2-mode (c) π-mode conditions.

3.4.2. PIC Simulation

The beam present simulation is performed using "CST Particle Studio", which is a commercial 3D PIC code. The simulation model is built using the design methodology given in section III, for 2.75 GHz frequency according to the design parameters are given in Table 3.1. The beam parameters given by Miller *et al*. [Miller *et al.* (1992)] for the experimental version of reltron are selected. The total beam voltage applied is 850 kV, out of which anode cathode gap is driven by 100 kV step voltage with 1ns rise time,

and the post-acceleration gap is driven with 750 kV step voltage with 1ns rise time. The initial beam current of 750 A at the cathode is applied. Explosive emission model with 1ns rise time is selected to emit the electrons. With these parameters, the simulation is performed for 100 ns duration.

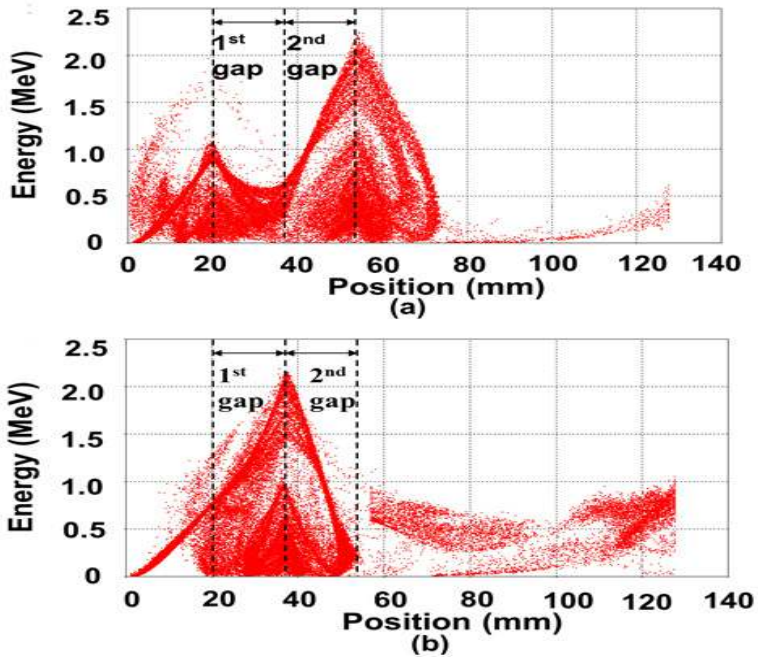

Figure 3.4: Plot of electron's phase space (a) first half cycle (b) second half cycle.

The electron beam bunching obtained after the PIC simulation is shown in Fig. 3.4, which shows that the electrons undergo a rapid acceleration in anode-cathode gap. In the first half cycle shown in Fig 3.4(a), as the electrons enter into the modulation cavity the deceleration of electrons in the first grid spacing and acceleration in the second grid spacing take place. This process gives the electrons a V-shape kinetic energy distribution in the modulation cavity. In the second grid spacing, the electrons experience a larger kinetic energy change as it leaves the modulation cavity. In the next half cycle shown in Fig 3.4(b), a Lorentz reversal force is experienced by the electrons and get accelerated in the first gap and decelerated in the second gap. The acceleration and deceleration processes lead to double velocity modulation in the modulation cavity. This velocity modulation generates highly bunched electron beam

and introduces an energy spread in the electron bunches. This energy spread is minimized through the application of post-acceleration gap which also increases the beam power [Soh (2012)].

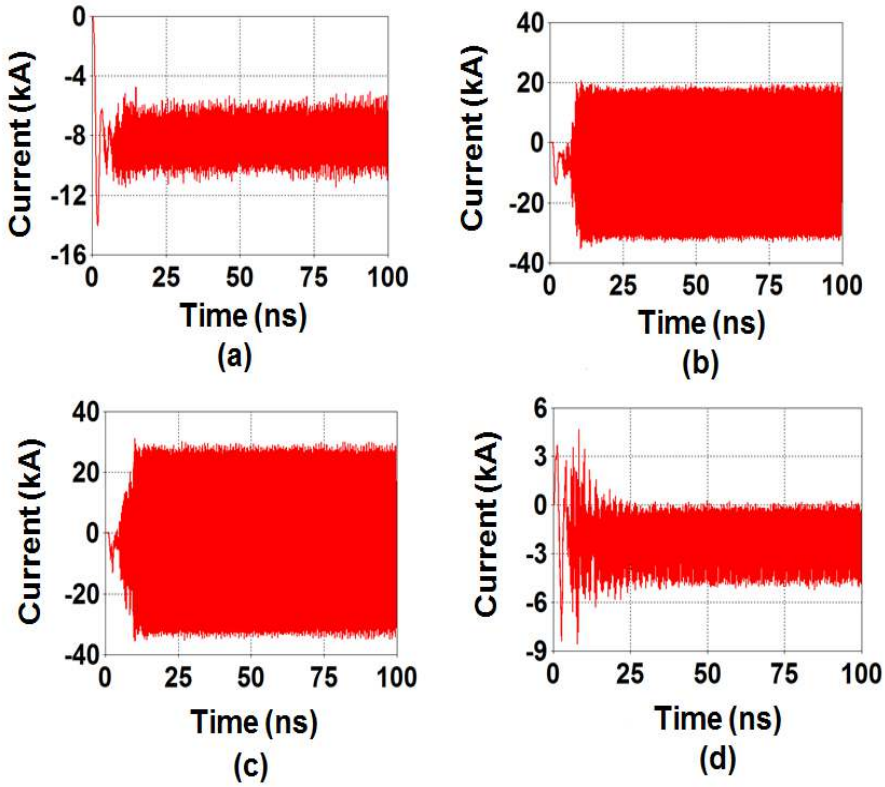

Figure 3.5: Current signal developed in **(a)** anode-cathode gap **(b)** first grid spacing in modulation cavity **(c)** second grid spacing in modulation cavity **(d)** post-acceleration gap.

In order to observe the current developed in different sections of the device, current monitors are used and plotted in Fig. 3.5. Initially, the current in the anode-cathode gap shown in Fig. 3.5(a) is developed through the explosive emission at the cathode. As the electrons enter into the modulation cavity, they undergo a current modulation, and the current developed in the first and second grid spacing of the modulation cavity, are shown in Fig. 3.5(b) and Fig. 3.5(c), respectively. The current signals in the modulation cavity section is very much higher than the anode-cathode gap current. These high currents in the modulation cavity are due to the shorting of radial space charge field by the transparent grids. It also indicates a strong beam wave interaction inside the modulation cavity. The generation of such a high current creates a

self-magnetic field in the cavity which in turn focuses the electron beam thereby the magnetic insulation condition is achieved without requirement of the externally applied DC magnetic field.

When the electron beam current exceeds the space-charge limiting current, virtual cathode formation takes place. In case of reltron, the negative part of the virtual cathode is being considered, because it appears only when the potential is depressed in the cavity [Dubinov *et al.* (2004), Champeaux *et al.* (2016)]. This process generates a high RF field which stops the beam alternately, and then accelerating the bunched beam out of the cavity as shown in Fig 3.4. The current at the post-acceleration gap shown in Fig. 3.5(d) is significantly lower than the modulation cavity, which indicates that no modulation occurs in the post-acceleration gap. It only helps in reducing the relative energy spread in the electron bunches.

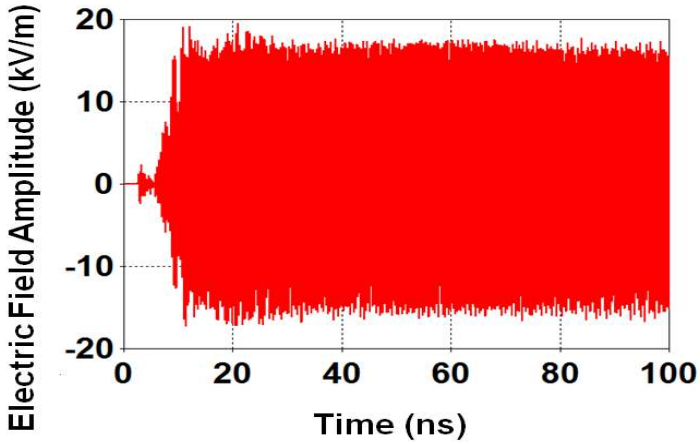

Figure 3.6: Electric field amplitude versus time plot at the output port.

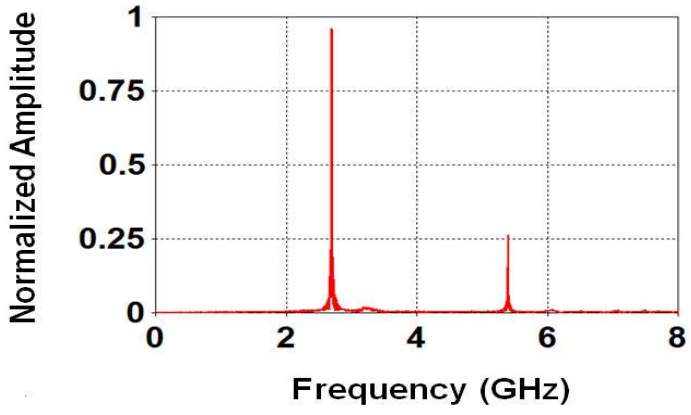

Figure 3.7: Frequency spectrum of electric field amplitude.

The electric field amplitude developed at the output cavity is shown in Fig. 3.6. The frequency spectrum is obtained by taking the Fast Fourier Transform (FFT) of the electric field. It can be seen from Fig. 3.7 that operating frequency is at 2.75GHz. By using a multiple output cavity instead of single output cavity, the amplitude level of second harmonic can be minimized. After electromagnetic simulation temporal RF output power is developed at TE_{10} mode as shown in Fig. 3.8. With the chosen beam parameters of Miller *et al*. [Miller *et al.* (1992)]: total beam voltage = 850kV, cathode voltage = 100kV, post-acceleration voltage = 750kV and beam current = 750A mentioned in Table 3.1, the RF output power developed through the present simulation is ~225MW, and the corresponding extraction efficiency is ~36%. The PIC simulation value obtained for the device efficiency are in agreement with the experimental results of Miller *et al*. [Miller *et al.* (1992)] within ~5%.

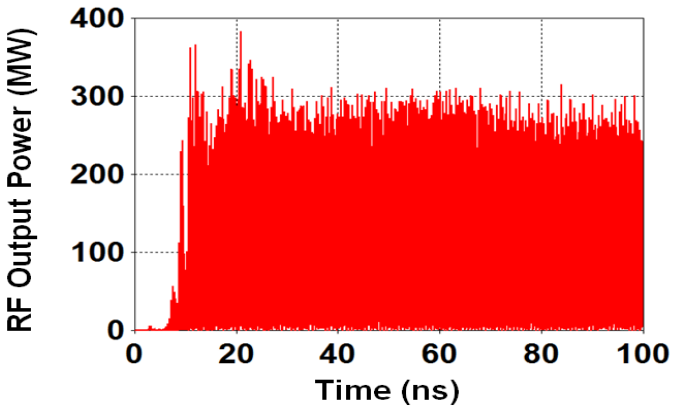

Figure 3.8: RF output power developed at the output port.

3.4.3. Parametric Analysis

The parametric analysis of reltron is also carried out using PIC simulation to study the sensitivity of the device to various beam parameters. The RF output power and efficiency variation has been observed for different cathode voltage and post-acceleration voltage. The dependence of RF output power and efficiency of the device

on the post-acceleration voltage with a static beam voltage of 100kV and beam current of 750A is examined as shown in Fig 3.9. At higher post-acceleration voltage, the RF output power of the device increases, this is due to the large reduction in the energy spread of the electron bunch and increase in the beam power. The overall phenomenon increases the efficiency of the device. An RF output power of ~370MW with ~50% efficiency has been obtained at 900kV post-acceleration voltage. The RF output power and efficiency as a function of cathode voltage are plotted in Fig. 3.10 with a constant post-acceleration voltage of 750kV and a beam current of 750A. It can be seen from Fig. 3.10 that the RF output power and efficiency of the device increase with the higher cathode voltages and provides a maximum RF output power of ~510MW with ~64% efficiency at a cathode voltage of 300kV. Hence, by increasing the cathode voltage the performance of the device can be improved.

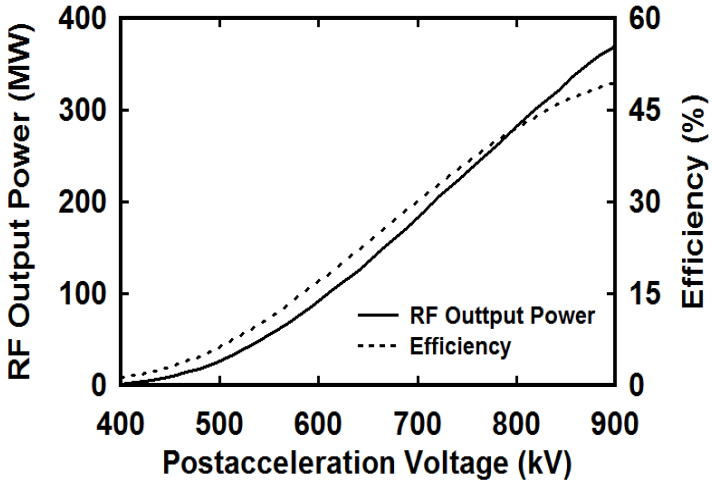

Figure 3.9: RF output power and efficiency as a function of post-acceleration voltage.

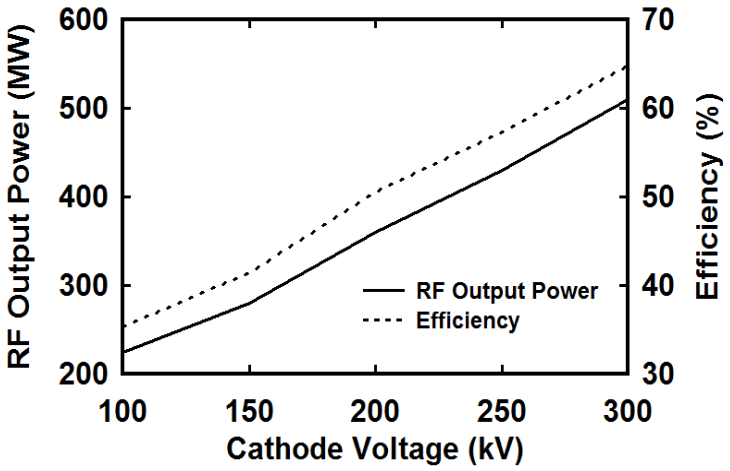

Figure 3.10: RF output power and efficiency as a function of the cathode voltage.

3.5. Conclusion

A detailed device description and an analytical study of start oscillation current of the HPM oscillator reltron has been presented along with the device design methodology. In order to validate the device design methodology and make comparisons with the reported experimental work, the beam parameters of 100 kV cathode voltage, 750 kV post-acceleration voltage and beam current of 750 A have been selected. The simulation results showed that the reltron produces an RF output power of ~ 225 MW with an extraction efficiency of ~ 36%. The results obtained have been found to be in agreement ~ 5% with previously reported experimental values. A parametric analysis through PIC simulation has also been made which suggests that at a higher cathode and post-acceleration voltage, the overall performance of the device increases.